ELSEVIER

Polymer 44 (2003) 495–501

polymer

www.elsevier.com/locate/polymer

Preparation and structure characterization of hairy nanoparticles consisting of hydrophobic core and thermosensitive hairs

Shinich Takata[a], Mitsuhiro Shibayama[a,*], Reiko Sasabe[b], Haruma Kawaguchi[b]

[a]*Neutron Scattering Laboratory, Institute for Solid State Physics, University of Tokyo, Tokai, Naka-gun, Ibaraki 319-1106, Japan*
[b]*Faculty of Science and Technology, Keio University, Hiyoshi, Yokohama 223-8522, Japan*

Received 29 May 2002; received in revised form 26 August 2002; accepted 17 September 2002

Abstract

Structural characterization of hairy nanoparticles consisting of poly(styrene-*co*-glycidyl methacrylate) (St/GMA) core and poly(NIPA-*co*-vinylimidazole) (NIPA/VIm) hair has been carried out by dynamic light scattering. The hairy molecules were introduced by surface graft-polymerization of a mixture of NIPA and VIm monomers to the St/GMA core particles with the hydrodynamic radius R_H of 135 ± 10 nm. The R_H of St/GMA-core-NIPA/VIm-hair particles was $R_H = 360 \pm 20$ nm at 20 °C, which gradually decreased to 285 ± 10 nm by heating to 33.0 °C, and then underwent a sharp decrease to 175 ± 10 nm by further heating to 33.8 °C. The final value went to 159 ± 10 nm at 36 °C. This decrease in R_H is due to the shrinking transition of NIPA/VIm chain by hydrophobic association. The degree of shrinking of the hairy particles is compared with that of bulk NIPA gels from the viewpoint of geometrical constraints.

Keywords: Nanoparticle; Dynamic light scattering; *N*-isopropylacrylamide

1. Introduction

Hairy nanoparticles are defined as the particles whose surface is covered with grafted linear polymer chains having high affinity with the dispersing medium. Hairy nanoparticles in water could be obtained by several methods such as (i) graft polymerization of hydrophilic monomer on core particles [1], (ii) coupling of existing water-soluble polymer with core particles [2], (iii) heterogeneous copolymerization of hydrophobic monomer with hydrophilic macromonomer, etc. [3–5].

Thermosensitive hair-carrying nanoparticles have gathered much attention so far because of a number of their possible applications [6–9]. *N*-isopropylacrylamide (NIPAM) is the most common monomer to give a thermosensitive polymer having a transition temperature, T_c, around 32–33 °C [10]. Matsuoka and coworkers successfully obtained poly-NIPAM (PNIPAM) hair particles by graft polymerization of NIPAM on OH function-carrying core particles using ceric ion by redox initiation mechanism at room temperature, at which the polymer formed in swollen state [11]. Although a discrete volume transition was anticipated, the PNIPAM hairs thus obtained did not respond discontinuously to the temperature change through 32 °C. The continuous response in a wide temperature range was attributed to two reasons: One was the loose clustering of NIPAM units, which starts from a temperature even lower than 25 °C, and the other was entanglement of chains restricting the sharp conformational change. Another reason, but probably the most essential reason, could be ascribed to the nature of PNIPAM chain itself as pointed out by Wu [12]. He carefully examined the coil-to-globular transition of linear chains and the volume phase transition of spherical microgel of PNIPAM and concluded that the former is not an all-or-nothing process and the latter is practically continuous. In order to bestow a capability of discrete transition, Matsuoka introduced a small amount of ionic groups to the hair molecules. They found that an introduction of less than 0.1% acrylic acid (AAc) was effective enough to lead to a sharp transition, but a larger amount of addition resulted in loss of sharp transition [13]. Hairy nanoparticles containing a small amount of vinylimidazole (VIm) were also prepared and a transition was successfully achieved [20].

In the previous papers [11,13], the temperature dependence of hydrodynamic diameter was measured for these hairy nanoparticles by dynamic light scattering (DLS) under

* Corresponding author. Tel.: +81-29-287-8904; fax: +81-29-287-3922.
E-mail address: sibayama@issp.u-tokyo.ac.jp (M. Shibayama).

0032-3861/03/$ - see front matter © 2002 Elsevier Science Ltd. All rights reserved.
PII: S0032-3861(02)00768-1

a limited experimental condition, which clearly showed a sharp transition of these hairy nanoparticles. However, focus was mainly placed on the synthesis of the hair particles and the structure was not extensively discussed from the viewpoint of molecular basis. In this study, a more quantitative study on the structure characterization was conducted as a function of temperature for these hairy nanoparticles with DLS technique.

2. Theoretical background

2.1. Dynamic light scattering

The dynamics of colloidal particles in aqueous solutions can be investigated by DLS. The intensity time-correlation function (ICF), $g^{(2)}(\tau)$, is given as a function of decay time,

$$g^{(2)}(\tau) \equiv g^{(2)}(\tau;q) = \frac{\langle I(0;q)I(\tau;q)\rangle_T}{\langle I(0;q)\rangle_T^2} = \beta|g^{(1)}(\tau;q)|^2 + 1 \quad (1)$$

where $\langle I(\tau;q)\rangle_T$ is the scattering intensity at time τ, $\langle\cdots\rangle_T$ denotes time average, and β is the coherence factor (<1). q is the momentum transfer defined by

$$q = (4\pi n/\lambda)\sin(\theta/2) \quad (2)$$

with the refractive index of the medium, n, the wavelength of the incident light, λ, and the scattering angle, θ. $g^{(1)}(\tau)$ is the scattering field ICF.

In general, $g^{(1)}(\tau)$ is a sum of relaxation functions with different characteristic-decay rate, Γ_i, and is given by

$$g^{(1)}(\tau) = \sum_i G(\Gamma_i)\exp(-\Gamma_i\tau)\Delta\Gamma = \int_0^\infty G(\Gamma)\exp(-\Gamma\tau)\mathrm{d}\Gamma \quad (3)$$

where $G(\Gamma)$ is the characteristic decay rate distribution function. The logarithm of $g^{(1)}(\tau)$ can be expanded to a power series of τ, which is so-called the cumulant expansion,

$$\ln g^{(1)}(\tau) = \sum_{m=1} \frac{K_m}{m!}(-\tau)^m = -K_1\tau + \tfrac{1}{2}K_2\tau^2 + \cdots \quad (4)$$

The coefficient, K_m, is related to the moments of the relaxation rate as are given by

$$K_1 = \langle\Gamma\rangle, \qquad K_2 = \langle\Gamma^2\rangle - \langle\Gamma\rangle^2, \qquad K_3 = \langle\Gamma^3\rangle - 3\langle\Gamma\rangle\langle\Gamma^2\rangle + 2\langle\Gamma\rangle^3 \quad (5)$$

Γ is related to the diffusion coefficient, D, i.e.

$$\Gamma = Dq^2 \quad (6)$$

In practice, the diffusion coefficient can be obtained directly from the initial slope of $\ln[g^{(2)}(\tau) - 1]$ vs τ as follows,

$$D_{\mathrm{app}} = -\frac{1}{2q^2}\frac{\partial}{\partial\tau}\ln[g^{(2)}(\tau;q) - 1] \quad (7)$$

The hydrodynamic radius of the particles, R_{H}, is then calculated with the Stokes–Einstein equation,

$$R_{\mathrm{H}} = \frac{kT}{6\pi\eta D} \quad (8)$$

where η, k, and T are the solvent viscosity, the Boltzmann constant, and the absolute temperature, respectively. The size distribution of the particles can be directly obtained by inverse Laplace transform of $g^{(1)}(\tau)$, because Eq. (3) shows that $g^{(1)}(\tau)$ is a Laplace transform of $G(\Gamma)$.

3. Experimental section

3.1. Materials

Styrene (St), glycidyl methacrylate (GMA) and divinyl benzene (DVB) were distilled under reduced pressures. *N*-isopropylacrylamide (NIPAM, Kojin Co.) was recrystallized from hexane–toluene (1/1 in volume basis). Potassium persulfate (KPS) was recrystallized from water at 40 °C. Vinyl imidazole (VIm) and ceric ammonium nitrate (Ce) were used as received.

3.2. Preparation of core particles

St-GMA copolymer particles were prepared by two-step emulsifier-free emulsion copolymerization at 70 °C under nitrogen. The polymerization recipe is shown in Table 1. The surface of the particles was found to be fully masked with poly(glycidyl methacrylate) which was partially hydrolyzed during the polymerization to glycelol methacrylate sequence as reported previously [14].

3.3. Preparation of hairy particles

Graft polymerization of NIPAM/VIm mixed monomers onto the core particles was carried out at 25 °C using Ce which is composed of a redox initiation system with glycerol groups on the core particles. The recipe of the graft polymerization is also presented in Table 1. The conversion

Table 1
Polymerization recipes

Core particle formation		Hairy particle formation	
St	1.20 g	Core particle	0.5 g
GMA (1st step)	1.80 g	NIPAM	3.73 g
DVB	0.04 g	VIm (or AAc)	0.0188 g
GMA (2nd step)	2.00 g	Buffer[a]	60 g
Water	110 g	Water	15 g
KPS/water	0.04 g	Ce/water	60 g

[a] Buffer HCl/CH_3COONa pH 3.48.

of the polymerization of PNIPAM was ca. 80%. The PNIPAM homopolymer was obtained in the aqueous medium by ca. 90% of polymer (2.8 g). The yield of PNIPAM hair on the core, estimated from the above values, was ca. 40% (0.2 g of hair for 0.5 g of St/GMA core).

3.4. Characterization of hairs

Latex particles settled by centrifugation were redispersed in water at pH 1 and stirred at room temperature for 3 days, by which the hair molecules were detached from the core. The dispersion containing PNIPAM chains released from the core particles were centrifuged. The supernatant was dialyzed for a week and then evaporated. The solid material was dissolved in acetone and precipitated in ether. Thus purified PNIPA chains were vacuum-dried before using for static light scattering. The molecular weight of the hair molecules was measured by a multi-angle light scattering instrument (SEC-MALLS, Shoko Tusho Co., Tokyo). The separation column and detector used were Shodex KD-806M and Wyatt DAWN EOS/Shodex RI-71. The moving solvent was 10 mM LiBr in DMF.

3.5. Characterization of particles

The characterization of the hair particles was carried out by transmission electron microscopy (TEM), and DLS. The size of dried particles was measured with a TEM (JSM-5200, JEOL Co.) On the other hand, the hydrodynamic radius, R_H, was measured by DLS as a function of temperature. A static/dynamic compact goniometer (SLS/DLS-5000), ALV, Langen, Germany, was used with a 22 mW He–Ne laser (the wavelength in vacuum; $\lambda = 632.8$ nm). The scattered photons were collected with a set of static/dynamic enhancer and avalanche photo diode system. The scattering angles were covered from 30 to 150°. The temperature of the sample was regulated within an error of ± 0.1 °C. Typical measuring time was 30 s. For scattering measurements, the stock solution with the solid content of 0.54 wt% was diluted by 5×10^3, 10×10^3, and 50×10^3 times.

4. Results and discussion

4.1. Size of dried particles

Fig. 1 shows the transmission electron micrographs of (a) the core particles and (b) hairy particles dried from a 0.01 wt% solution at room temperature. The average diameters were 204 and 237 nm, respectively. The difference 33 nm corresponds to the double of the thickness of contracted layer of PNIPAM graft chains on the surface of the core particle. The diameter of hairy particles dried at 40 °C was also 237 nm, which was the same as the diameter of the hairy particles dried at room temperature. This indicates that shrinkage took place to form a dense skin layer on the particle even if the particles were dried up at room temperature.

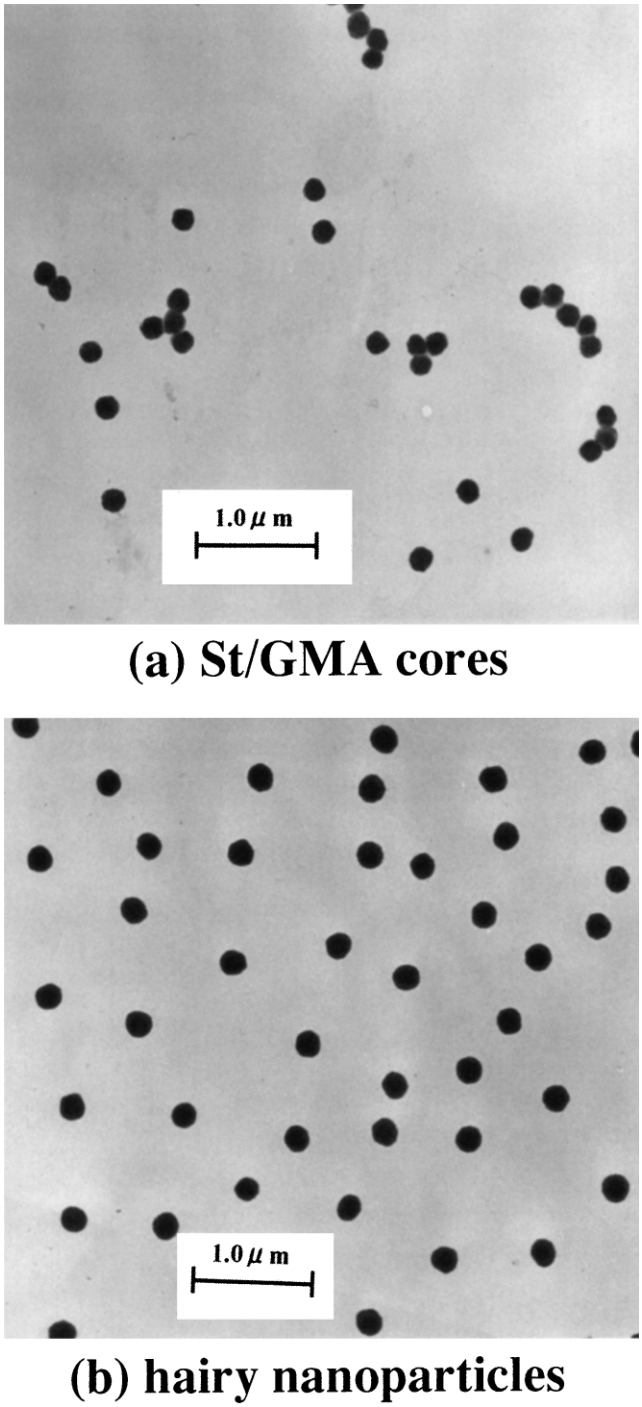

Fig. 1. Transmission electron micrographs of (a) St/GMA cores and (b) St/GMA-core-NIPA/VIm-hairy particles.

It should be also noted the following. Fig. 1b indicates a unique feature, that is, the particles are widely spread in the space without aggregation. This indicates that the hairy nanoparticles have a repulsive interaction to each other in a solution due to the excluded volume effect and electrostatic

interaction between the charges of VIm ions of the hairy molecules. The lower bound of the inter-particle distance may be related to the double of thickness of swollen PNIPAM hair layer at a given polymer concentration. The expected process to form such a structure in the hairy nanoparticles is as follows. It is deduced that a drying process started by anchoring the one side of the nanoparticle onto a grid of TEM. This anchoring preserves the distance between the nanoparticles. Only the hairy chains are shrunken by evaporation of the solvent, resulting in a widely separated arrangement of particles with a lower cut of the inter-particle distance (≈double of the size of the harily chains in the swollen state). Note that, such an arrangement was not observed in the process of the core particles, where the individual particles have a tendency to coagulate because of the absence of such a repulsive interaction (Fig. 1a).

4.2. Dynamic light scattering

Fig. 2 shows the time-intensity correlation functions (ICF), $g^{(2)}(\tau) - 1$, of St/GMA core particles at 20 and 35 °C, and the hairy particles at 20 and at 35 °C. All of these functions exhibit a single decay around, $\tau = 1.9$ ms (St/GMA core particles at 20 °C), $\tau = 1.2$ ms (St/GMA core particles at 35 °C), $\tau = 5.4$ ms (the hairy particles at 20 °C), and $\tau = 1.3$ ms (hairy particles at 35 °C). Note that the difference in the ICF between the St/GMA particles at 20 and 35 °C is due to the difference in the solvent viscosities between these temperatures. The size of the St/GMA particles is essentially invariant with respect to temperature as will be discussed later. The hydrodynamic radius R_H for St/GMA particles was evaluated to be 135 ± 10 nm at both 20 and 35 °C. The values of R_H for the hairy nanoparticles were 360 ± 20 nm at 20 °C, and 175 ± 10 nm at 35 °C. Another interesting feature in Fig. 2 is the scattering of the correlation at small-τ and lower coherence (i.e. values of the coherence factor, β) for the St/GMA core particles. This may indicate that the St/GMA core particles are less stable than the hairy particles due to lack of charges and/or hair molecules.

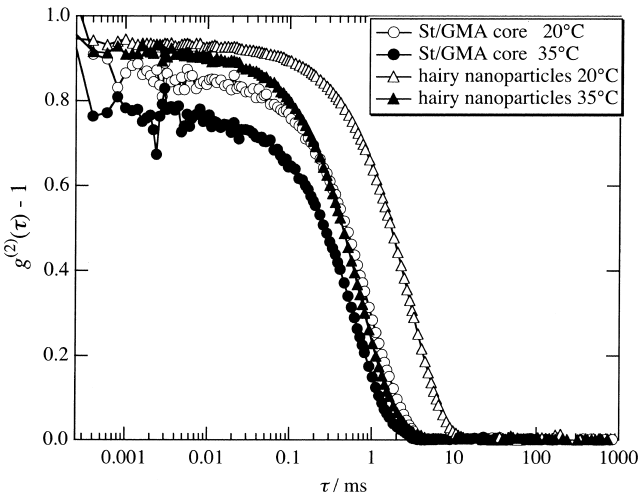

Fig. 2. The time-intensity correlation functions (ICF), $g^{(2)}(\tau) - 1$, of (a) St/GMA core particles at 20 and 35 °C, and (b) the hairy particles at 20 and 35 °C.

Fig. 3(a) shows the size distribution functions of the St/GMA core particles at 20 and 35 °C, and the hairy particles at 20 and at 35 °C obtained by CONTIN analysis [15]. As shown in the figure, the distribution functions are very sharp both for the St/GMA and the hairy nanoparticles. Note that the peak shifts toward the larger size side by introduction of the hair chains and toward the smaller size by heating. The latter is partially ascribed to the lowering of the solvent viscosity as described earlier. Fig. 3(b) shows plots of $G(\Gamma)$ vs $q^2/\Gamma\eta$, where the effect of the viscosity change by temperature is taken into account. It is clear from the plots that a significant increase in the particle size is observed for the hairy particles at 35 °C, while the others remain close to each other. The values of R_H evaluated from the peak

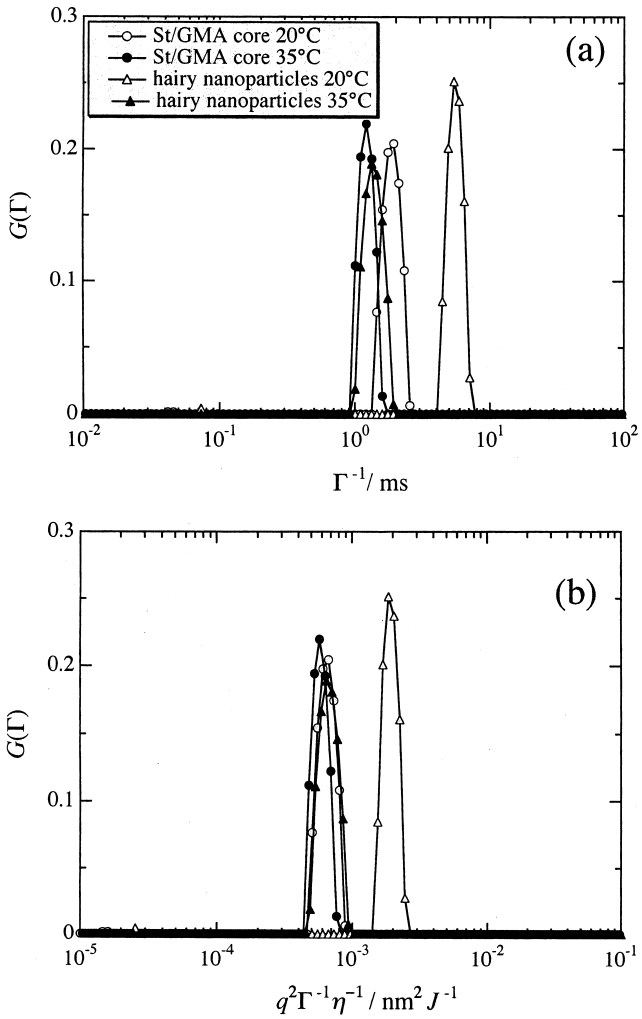

Fig. 3. (a) The size distribution functions of St/GMA core particles at 20 and 35 °C, and the hairy particles at 20 and 35 °C. (b) $G(\Gamma)$ vs $q^2/\Gamma\eta$ plots of the same systems, in which the temperature effect on viscosity is taken into account.

positions were in good accordance with those obtained from the initial slope of $\ln[g^{(2)}(\tau) - 1]$.

Fig. 4 shows the θ and concentration dependence of R_H for the hairy nanoparticles. The concentrations of the hairy nanoparticles were varied from 1.08×10^{-5} to 1.08×10^{-4} wt%. The nominal diffusion coefficient is known to be a function of concentration, C, as is given by Brown [16],

$$D = D_0(1 + k_D C + \cdots) \quad (9)$$

where k_D is a constant. Fig. 4 shows, however, no concentration dependence in D. Therefore, we conclude that the concentrations employed in this work are low enough for the evaluation of the hydrodynamic radius. Hence, we employ the R_H values obtained at $C = 1.08 \times 10^{-4}$ wt% in the following analysis.

Fig. 5 shows the temperature dependence of R_H for the hairy particles at $C = 1.08 \times 10^{-5}$ wt%. The values of R_H were obtained with a step of 0.2 °C in the range where R_H changed drastically. By increasing temperature, R_H gradually decreased from 360 ± 20 nm at $T = 20$ °C to 285 nm by heating to 33.0 °C, and then underwent a sharp decrease to 174 ± 10 nm by further heating to 33.8 °C. This sharp decrease in R_H is due to the hydrophobic dissociation of NIPA/VIm hair molecules. The dashed line in the figure denotes the R_H value for the St/GMA core.

Wu made a comparison of the volume changes of linear PNIPAM chains and PNIPAM microgels [12]. He claimed that the coil-to-globule transition of linear PNIPAM chains is not an all-or-none transition and the chain shrinks gradually with increasing temperature. The volume phase transition of PNIPAM microgels also exhibited a continuous transition unlike a bulk PNIPAM gel undergoing a discrete transition. He explained that this continuous transition was due to a smaller contribution of the shear modulus in microgels than in a bulk PNIPAM gel. The volume phase transition of core-shell particles consisting of poly-St core and PNIPAM gel layer have

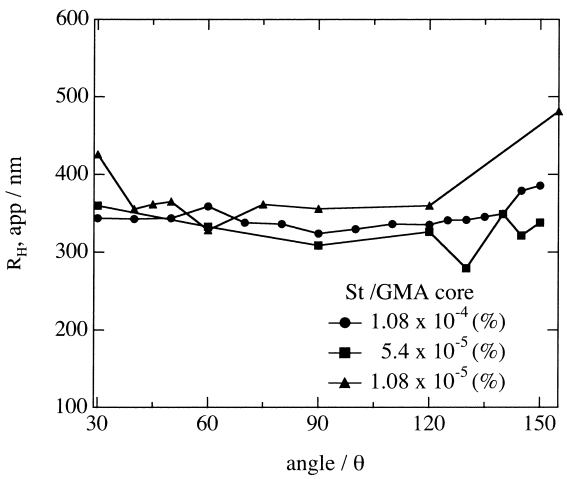

Fig. 4. The scattering angle, θ, dependence of the apparent hydrodynamic radius, $R_{H,app}$, for St/GMA core at various concentrations.

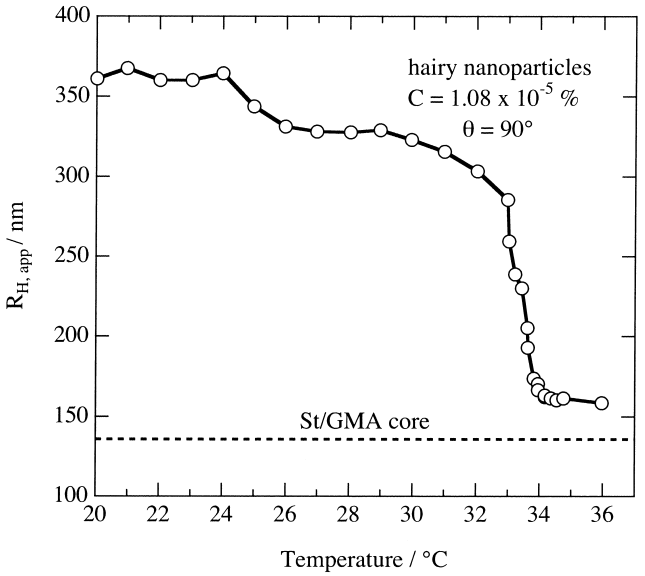

Fig. 5. The temperature dependence of the apparent hydrodynamic radius, $R_{H,app}$, of the hairy particles at $C = 1.08 \times 10^{-5}$ wt%.

been extensively investigated by Ballauf and coworkers [17–19]. They prepared a core-shell latex of which shell was made of PNIPAM microgels and investigated the volume phase transition of the shell by means of small-angle X-ray scattering, DLS, and small-angle neutron scattering. They studied the volume transition of a core shell latex particles of St-core covered by cross-linked PNIPAM chains with 2 mol% ionization by acrylic acid [18]. The radius of St core was 59 nm and the change of the corona by volume transition was $\Delta R_H \approx 100$ nm. The change in the R_H near the transition temperature is rather broad compared with the hairy particles studied here (Fig. 5) even though the latter had a charged shell molecules with less ionization (0.5 wt%) [20]. They concluded that the transition is continuous and the degree of shrinking is highly suppressed due to the geometrical confinement, i.e. affixing of one chain to the core and shrinking only along the radial direction being allowed. Since a continuous volume phase transition was also observed even for a partially charged PNIPAM shell surrounding St core [18], this geometrical-confinement effect seems to be quite large. However, as shown in this study, the transition of the NIPA/VIm hairs anchored to St/GMA particles is quite sharp with respect to temperature if there are no cross-links are present in the hair chains. Hence, the presence of cross-links is essential for the suppression of the degree and sharpness of shrinking.

Table 2 shows the sizes of particles of the St/GMA core, the hairy particle (i.e. core + hair) in the dried state, the hairy particle in the shrunken state, and the hairy particle in the swollen state. The core size obtained by TEM is somewhat smaller than those obtained by DLS, which may be due to shrinking of the core by drying process. The difference in the sizes between the (core + dried hair) and core corresponds to the dried layer of PNIPA/VIm. The

Table 2
Comparison of the radii of particles and layer thicknesses

Method	Radii of particles (in nm)				Layer thickness (in nm)	
	Core	Core + dried hair	Core + shrunken hair	Core + swollen hair	shrunken–core	swollen–core
EM	102 ± 10	118 ± 10	–	–		
DLS	135 ± 10	–	159 ± 10	360 ± 20	24 ± 2	225 ± 10

change in the particle sizes evaluated by DLS upon the temperature change is quite large, indicating a shrinking/swelling of the hair chains.

5. Comparison of the coil–globule transition of the hairy molecules with the volume phase transition of PNIPA gels

Now, let us discuss the change of the layer thickness of the hairy molecules, which is essentially a temperature-induced coil–globule transition of PNIPA chains. Fig. 6 schematically shows the hairy nanoparticles at low (left; $T < T_c \approx 33.3\,^{\circ}C$) and high temperatures (right; $T > T_c$), which is illustrated on the basis of the data taken by DLS. As shown here, the layer thickness changes drastically as large as 225 ± 10 nm by simply changing temperature (Table 2). The molecular weight and the z-average radius of gyration of the free PNIPAM molecules (at 25.0 °C in dimethyl formamide with 10 mM LiBr), R_z, were evaluated by static light scattering to be 2.4×10^6 and 77 nm, respectively. Hence, the value of R_z is much smaller than the observed hair length in the swollen state (225 nm). This means that the hair chain is highly stretched along the radial direction as shown in the left cartoon of Fig. 6. This may be due to electrostatic repulsion between hair chains because of anchoring the one end of the hair molecule on the surface of the core.

The volume of the layer occupied by the hairy chains are easily evaluated by,

$$V_{\mathrm{hair,sw}} = \frac{4\pi}{3}(R_{\mathrm{sw}}^3 - R_{\mathrm{core}}^3)$$

$$V_{\mathrm{hair,sh}} = \frac{4\pi}{3}(R_{\mathrm{sh}}^3 - R_{\mathrm{core}}^3)$$

where R_{sw}, R_{sh}, and R_{core} are the radius of the hairy particles in swollen and shrunken states, and the core radius. The evaluated values are $V_{\mathrm{hair,sw}} = 1.85 \times 10^8$ and $V_{\mathrm{hair,sh}} = 6.53 \times 10^6$ nm^3 in the swollen (sw) and shrunken (sh) states, respectively. These values readily lead to the estimation of the local volume fraction of the hairy molecules in swollen and shrunken states; $\phi_{\mathrm{sw}} = 0.013$, $\phi_{\mathrm{sh}} = 0.37$, which are reasonable values for PNIPAM gels in swollen and shrunken states, respectively. The value of $\phi_{\mathrm{sw}} = 0.013$ is very close to the case of PNIPAM gel prepared with 200 mM of NIPAM monomer and 2.50 mM

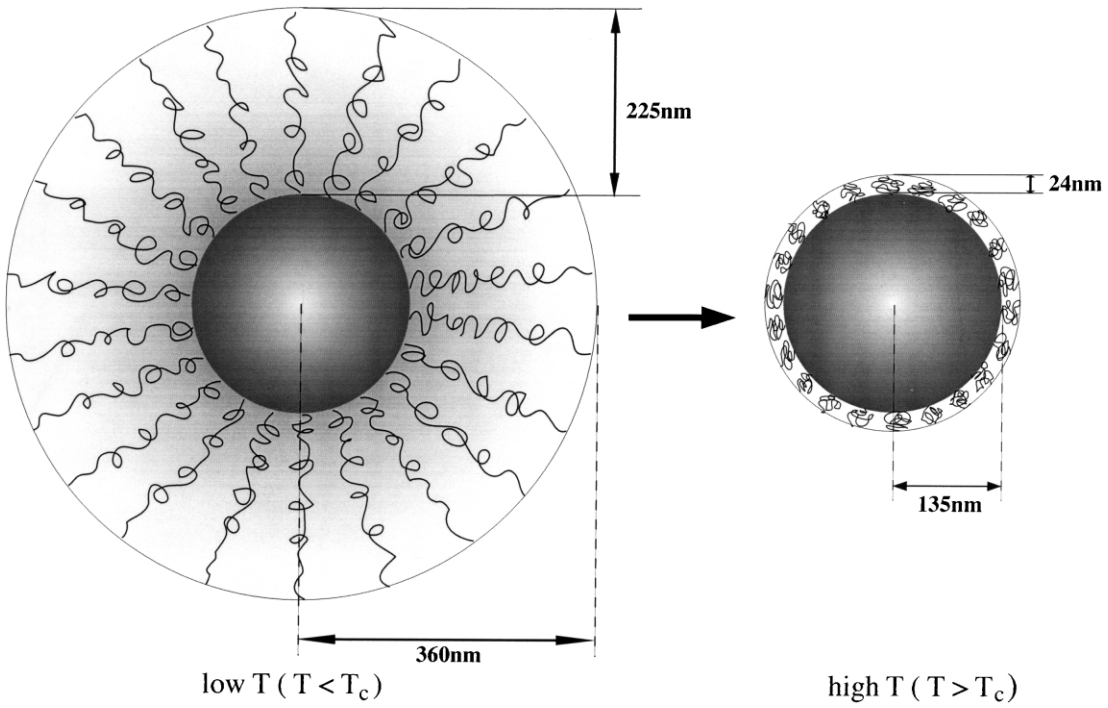

Fig. 6. Schematic illustrations showing the relative sizes of the hairy nanoparticles in swollen (left) and shrunken states (right).

of cross-linker (*N*,*N*′-methylenebisacrylamide). The equilibrium volume fraction of the polymer at swelling equilibrium at 20 °C was $\phi_{sw} = 0.012$ [21] and $\phi_{sh} = 0.67$ [22]. Hence, the relative volume change upon shrinking transition is estimated to be 28 (for the hairy PNIPAM) which is much larger than that of thermosensitive bulk PNIPAM gels (≈15). It is needless to mention that this is partially due to the anisotropic swelling/shrinking by anchoring one side of the hairy molecule to the core particle.

5.1. Estimation of the hair density on the surface and packing problem of the hair chains in shrunken and swollen states

The density of the hair molecules on the surface can be evaluated with the data of the sizes of the bare particle core and the hairy particles in the dried state (Table 2) and the molecular weight. By approximating the bulk density of the NIPA/VIm being 1 g/cm^3, we evaluated the volume ratio of the NIPA/VIm hair to the core particles and the number of hair chains partitioned to be 0.35 and 587, respectively. Note that the former is in reasonably good agreement with that evaluated by synthesis (≈40%). This leads to an estimation of the occupied area by a hair chain on the core surface to be of 15^2 nm^2/molecules. Hence, each chain is apart by about 15 nm to each other. This value is much smaller than the radius of gyration of the PNIPAM chain in free state (≈79 nm). This discussion also indicates that the hair chain has to be highly stretched out along the radial direction, resulting in forming a thick layer on the core (≈225 nm). On the other hand, the surface density of the hair molecules is much lower than that of block copolymer micelles in a selective solvent (≈3^2 nm^2/molecules) [23]. This is due to the fact that in the case of graft polymerization the surface density is tunable unlike the case of block copolymers.

6. Conclusion

Structural characterization of hairy nanoparticles consisting of poly(styrene-*co*-glycidyl methacrylate) (St/GMA) core and poly(NIPAM-*co*-vinylimidazole) (NIPAM/VIm) hair chains has been carried out by DLS as well as by electron microscopy. The electron micrographs clearly indicate formation of spherical particles. The core particles tend to aggregate by drying, whereas the hairy nanoparticles keep apart to each other due to repulsive interaction of the hair molecules.

The R_H of the hairy nanoparticles was $R_H = 360 \pm 20$ nm at 20 °C. R_H gradually decreased to 285 ± 10 nm by heating to 33.0 °C, and then underwent a sharp transition to 174 ± 10 nm by further heating to 33.8 °C and finally reached the value of 159 ± 10 nm at 35.0 °C. This decrease in R_H is due to the shrinking transition of NIPAM/VIm chain by hydrophobic dissociation. The transition was pseudo-discontinuous. The size of the hair chains is much larger than that expected for unperturbed chains. This means that the hair chains are highly stretched along the radial direction due to the geometrical constraint by anchoring one side of the hair chain to the core particle. The change of hair chains upon transition was up to 28 times, which is much larger than the corresponding PNIPAM gels. This also indicates that the anisotropic swelling/shrinking leads to a larger swelling ratio. These differences are explained with the absence/presence of cross-links. That is, cross-links reduce both the degree of shrinking and sharpness of the transition with respect to temperature. It is concluded the hairy nanoparticles are quite suitable as a high temperature-sensitive nanomaterials for various applications.

Acknowledgements

This work is partially supported by the Ministry of Education, Science, Sports and Culture, Japan (Grant-in-Aid, 12450388 and 13031019 to M.S.).

References

[1] Zhu PW, Napper DH. J Colloid Interface Sci 1996;177:343.
[2] Yasui M, Shiroya T, Fujimoto K, Kawaguchi H. Colloid Surface 1997;8:311.
[3] Hoshino F, Sakai M, Kawaguchi H, Ohtsuka Y. Polym J 1987;19:383.
[4] Kitano H, Kawabata J. Macromol Chem Phys 1996;197:1721.
[5] Chen M-Q, Kishida A, Akashi M. J Polym Sci, Polym Chem 1996;34:2213.
[6] Pelton RH, Chibante P. Colloid Surface 1986;20:247.
[7] Snowden MJ, Marston NJ, Vincent B. Colloid Polym Sci 1994;272:1273.
[8] Oh KS, Oh JS, Choi HS, Bae YC. Macrmolecules 1998;31:7328.
[9] Duracher D, Elaissari A, Mallet F, Pichot C. Macromol Symp 2000;150:305.
[10] Shild HG. Prog Polym Sci 1992;17:163.
[11] Matsuoka H, Fujimoto K, Kawaguchi H. Polym Gels Network 1998;6:319.
[12] Wu C. Polymer 1998;39:4609.
[13] Matsuoka H, Fujimoto K, Kawaguchi H. Polym J 1999;31:1139.
[14] Matsuoka H, Fujimoto K, Kawaguchi H. Polym J 2001;31:1139.
[15] Provencher SW. Comp Phys Commun 1982;27:213. See also p. 229.
[16] Brown W. Macromolecules 1991;24:5151.
[17] Dingenouts N, Norhausen C, Ballauff M. Macromolecules 1998;31:8912.
[18] Kim J-H, Ballauff M. Colloid Polym Sci 1999;277:1210.
[19] Seelemeuer S, Deike I, Rosenfeldt S, Norhausen C, Dingenouts N, Ballauff M. J Chem Phys 2001;114:10471.
[20] Kawaguchi H, Isono Y, Sasabe R. ACS Symp Ser 2002;.
[21] Shibayama M, Shirotani Y, Shiwa Y. J Chem Phys 2000;112:442.
[22] Shibayama M, Shirotani Y, Hirose H, Nomura S. Macromolecules 1997;30:7307.
[23] Shibayama M, Hashimoto T, Kawai H. Macromolecules 1983;16:16.